

Bethe-Salpeter study of radially excited vector quarkonia

V. Šauli*

Department of Theoretical Physics, Institute of Nuclear Physics, CAS, Rez near Prague 250 68, Czech Republic
(Received 23 December 2011; published 8 November 2012)

We solve the Bethe-Salpeter equation for a system of a heavy quark-antiquark pair interacting with a Poincare invariant generalization of screened linear confining potential. In order to get a reliable description the Lorentz scalar confining interaction is complemented by the effective one gluon exchange. Within the presented model we reasonably reproduce all known radial excitations of the vector charmonia. We have found that J/Ψ is the only charmonium left below naive quark-antiquark threshold $2m_c$, while the all excited states are situated above this threshold. We develop a method which is able to provide a solution of full four dimensional Bethe-Salpeter equation for the all excited states. We discuss the consequences of the use of the free propagators for calculation of excited states above the threshold. The Bethe-Salpeter string breaking scale $\mu \simeq 350$ MeV appears to be relatively larger than the one defined in various potential models $\mu \simeq 150$ MeV.

DOI: [10.1103/PhysRevD.86.096004](https://doi.org/10.1103/PhysRevD.86.096004)

PACS numbers: 11.10.St, 11.15.Tk

I. INTRODUCTION

Excited meson spectroscopy is a keystone experimental output, which is essential for understanding of quark-antiquark interaction. The dynamics of meson constituents is driven by solely known strongly interacting quantum field theory—quantum chromodynamics. The explanation of quarks and gluons confinement is one of the great challenges of the theory of strong interaction. The same confining forces are responsible for a large degeneracy which emerges from the spectra of the angularly and radially excited resonances. As reported in Refs. [1–4] such degeneracy is observed in $p\bar{p}$ annihilation by the Crystal Ball collaboration at LEAR in BERN [5]. Similar can be deduced from heavy quarkonia production in e^+e^- annihilations. Recently, *BABAR*, Belle, BESS, and LHCb experiments continue collection of various meson experimental data.

Following ideas of Ref. [6], confinement in heavy flavor sector has typically been associated with a linearly rising potential between constituents [7]. The spin degeneracy observed in heavy quarkonia spectrum tell us that the main part of confining interaction should be largely spin independent. A various lattice fits led to various predictions for the potential between quark-antiquark states. A well-known Cornell parametrization of the static Wilson loop derived potential [8,9],

$$V(r) = -\alpha/r + \sigma r \quad (1)$$

has appeared to be suited for description of the first few excited mesons.

Recently in Refs. [10–12] it has been found that the meson spectroscopy is better described by “confining” potential which is bounded from above. While in the absence of dynamical quarks the nonrelativistic static

potential can eventually show up a linear asymptotic, it should be flattened in large distance due to the string breaking associated with light hadron productions. In this respect, the exponential potential can be regarded as a screened version of the linear potential. The screening effect should be universal, e.g., scheme and gauge independent property of low energy QCD as the creation of the light quark-antiquark pairs is energetically favorable and pions and other light mesons is observable fact. The screening could be included in order to explain observed hierarchy of radially excited heavy mesons. Obviously, the spectrum deviates from the linear Regge trajectory, for a proposal of 5s and 6s charmonium candidate see Ref. [13], however recall the deviation from the linear Regge trajectory is expected in the light meson sector as well [14].

The Coulombic part of the potential is naturally expected in QCD, however as shown recently, it can be suppressed in the charmed meson sector by a not yet understood mechanism [15]. Furthermore, it is related with gluon exchange then screening of Coulomb potential is expected as well. This more subtle matter could be related with soft gluon mass generation [16,17] through the Yang-Mills Schwinger mechanism. Actually the dynamical gluon mass generation is suggested by finiteness of the lattice gluon propagator in the deep infrared, for the recent lattice data on gluon propagator in Landau gauge see Ref. [18]. We expect the screening mass characterizing string breaking and the soft gluon mass have similar size $\simeq \Lambda_{\text{QCD}}$.

For bound states which lie above the naive quark-antiquark threshold, the Bethe-Salpeter equation (BSE) kernel becomes singular, which causes many usual numerical treatments to fail and/or become impossible in practice. To the author’s knowledge, a plethora of solutions have been obtained in relativistic quantum mechanics [19] or by solving various phenomenological 3D reduction of BSE [20,21],

*sauli@ujf.cas.cz

however comparison with the original BSE is completely missing. The way of three-dimensional reduction of the BSE is rather arbitrary and difficult to control without keeping the solution of the original BSE. Actually, choice of 3d equation has a large effect already for the ground states. In the study [20] 200 MeV difference between equal time and certain quasipotential equation has been found for the charmonium ground state $l = 0$. This increases slightly for higher l as well. The differences between Schrödinger and 3d approximated BSE spectra appears to be more significant for higher excited states, where following Ref. [20] the difference has been estimated $M_{\text{QM}} - M_{\text{ET}} \simeq 300$ MeV for $l = 4, 5$ charmonia. The comparison between various relativistic approximations has not been studied for radially excited states, however we expect very similar effects there. From all this is apparent that relativistic covariance is important for charmonium and it will be useful to have the solution without any 3d approximation. Due to this reasoning, using single component approximation, but keeping the full four dimensionality of BSE we study the effect of retardation in the slopes of radially excited vector mesons. The experimental knowledge of heavy vector quarkonia is the main reason why we concern spin 1 mesons as a first (as time is being the pseudoscalars have been computed already in Ref. [22]).

II. KERNEL FOR BETHE-SALPETER EQUATION

In the quantum field theory the two body bound state is described by the three-point bound state vertex function, or equivalently by the Bethe-Salpeter amplitude. Both of them are solutions of the corresponding covariant four-dimensional BSE [23]. In principle, common framework of Schwinger-Dyson and BSEs offers unique Poincare invariant generalization of the quantum mechanical picture sketched above, however practical solutions are always incomplete due to the truncation of the equations system. Because of this fact we rather phenomenologically estimate what should be the form of the BSE kernels here. In this paper we use “confining” interaction kernel of the form

$$V_s(q) = \frac{C}{(q^2 - \mu^2)^2}; \quad (2)$$

which is certain screened form of $\simeq 1/q^4$ scalar interaction. The remaining considered part of the interaction kernel has the Dirac decomposition identical with the one gluon exchange $\simeq \gamma_{\alpha\beta}^\mu V_\nu \gamma_{\alpha'\beta'}^\nu$.

For clarity we write down the BSE completely here

$$S^{-1}(q + P/2)\chi(p, q)S^{-1}(q + P/2) = -i \int \frac{d^4k}{(2\pi)^4} \gamma_\mu \chi(k, P) \gamma_\nu G^{\mu\nu}(k - q) - i \int \frac{d^4k}{(2\pi)^4} \chi(k, P) V_s(k - q); \quad (3)$$

$$G^{\mu\nu}(k - q) = g^{\mu\nu} V_\nu = \frac{g^2 g^{\mu\nu}}{(k - q)^2 - \mu_g^2}.$$

Two scalar functions V_s and V_ν in (3) complete our simple Poincare invariant generalization of quantum mechanical potentials. Here, clearly $G^{\mu\nu}$ represents effective gluon propagator in Feynman like gauge, where the effective soft gluon mass μ_g has been introduced. The double pole scalar interaction V_s leads to regular exponential potential in the position space. Actually, in heavy quark limit one can consider three-dimensional potential

$$V_s^{\text{QM}}(\vec{k}) = \int_0^\infty dr \frac{4\pi r \sin(kr)}{k} V(r) = \sigma \frac{-8\pi}{(\vec{k}^2 + \mu^2)^2}, \quad (4)$$

where the potential in position space reads

$$V(r) = -\sigma \frac{e^{-\mu r}}{\mu}. \quad (5)$$

Thus in a certain sense the BSE model considered in this paper represents relativistic generalization of the models considered in Refs. [10, 11]. S in Eq. (3) stands for charm quark propagator, which in our simplest approximation is taken as

$$S^{-1}(l) = \not{l} - m_c, \quad (6)$$

and χ_V represents the Bethe-Salpeter wave function which has the general form:

$$\chi_V(q, P) = \not{\epsilon} \chi_{V0} + \not{P} \epsilon \cdot q \chi_{V1} + \not{q} \epsilon \cdot q \chi_{V2} + \epsilon \cdot q \chi_{V3} + [\not{\epsilon}, \not{P}] \chi_{V4} + [\not{\epsilon}, \not{q}] \chi_{V5} + [\not{q} \not{P}] \chi_{V6} + i \gamma_5 t \chi_{V7}, \quad (7)$$

with $t_\mu = \epsilon_{\mu\nu\alpha\beta} q^\nu P^\alpha \epsilon^\beta$, $\epsilon^2 = -1$, $\epsilon \cdot P = 0$.

Munczek and Jain [24] have shown that $V0$ component is dominant for the all ground state mesons, which dominance is particular for mesons made from heavy flavor (anti)quarks. The same is valid for the case of all pseudoscalar radial excitations [22], which strongly argue for that if there is a dominant component it stays to be the dominant one for higher excited states independently on the meson spin. Therefore we assume the same applies for excited vectors here, and we neglect all other components in the presented study.

Within the approximation, the Bethe-Salpeter equation in the rest frame reads

$$\chi_{V0}(p_E, P) = \frac{-p_E^2 - m^2 - P^2/4}{(-p_E^2 - m^2 + M^2/4)^2 + q_4^2 M^2} I_0, \quad (8)$$

where

$$I_0 = - \int \frac{d^4 k_E}{(2\pi)^4} [-2V_v + V_s] \chi_{V0}(k_E, P);$$

$$V_v = \frac{g^2}{q_E^2 + \mu^2}; \quad V_s = \frac{C}{(q_E^2 + \mu^2)^2}, \quad (9)$$

where we have performed Wick rotation into the Euclidean space. For Euclidean momenta we use the convention $k_E = (k_4, \vec{k})$, $k_E^2 = k_4^2 + \mathbf{k}^2$, while the total momentum is kept timelike $P^2 = -P_E^2 = M^2$ as required for the bound states. An extra problem arises for bound states which are heavier than the sum of constituents quark masses. As we are using propagators with single real poles, the Bethe-Salpeter wave function becomes singular since it is proportional to the product of the quark propagators. For the vertex function, the thresholdlike singularity should appear for the solution with $P^2 > 4m_q^2$. Because of this fact, the numerical integration requires special numerical care and we found it very advantageous to define the following auxiliary function

$$A(p_E, P) = \chi_{V0}(p_E, P) G_A(k, P),$$

$$G_A(k, P) = \left[\frac{p_E^2 + m^2 + P^2/4}{(-p_E^2 - m^2 + M^2/4)^2 + p_4^2 M^2 + \epsilon^4} \right]^{-1}, \quad (10)$$

where ϵ is a small regulator mass satisfying $\epsilon^4 \ll p_4^2 M^2$. Within the numerics the regulator can be limited to zero. In the limiting case we should add the residuum contribution stemming from the propagator pole. In the presented study we keep the regulator always finite and we neglect the residuum as well. It avoids complicated analytical continuation to the Minkowski space in this case.

Finally we integrate over the angles of 3d momentum subspace. Explicitly written, the BSE (8) reads

$$A(p_E, P) = \int_{-\infty}^{+\infty} \frac{dk_4}{(2\pi)} \int_0^\infty d\mathbf{k} \mathbf{k}^2 A(k_E, P) G_A(k, P)$$

$$\times \int \frac{d\Omega_{3d}}{(2\pi)^3} [-2V_v + V_s], \quad (11)$$

which can be finally rewritten as

$$A(p, P) = \int_{-\infty}^\infty dk_4 \int_0^\infty d\mathbf{k} A(k, P) G_A(k, P) [K_s + K_v];$$

$$K_s = \frac{C}{(2\pi)^3} \frac{\mathbf{k}^2}{[k_E^2 + p_E^2 - 2k_4 p_4 + \mu^2]^2 - 4\mathbf{k}^2 p^2};$$

$$K_v = - \frac{g^2}{(2\pi)^3} \frac{\mathbf{k}}{\mathbf{p}} \ln \left[\frac{k^2 + p^2 - 2k_4 p_4 - 2\mathbf{k}\mathbf{p} + \mu^2}{k^2 + p^2 - 2k_4 p_4 + 2\mathbf{k}\mathbf{p} + \mu^2} \right], \quad (12)$$

where the functions $K_{v,s}$ stem from Ω integration:

$$-2 \int \frac{d\Omega_{3d}}{(2\pi)^4} V_v = K_v, \quad \int \frac{d\Omega_{3d}}{(2\pi)^4} V_s = K_s. \quad (13)$$

III. NUMERICAL SOLUTION OF THE CHARMONIUM BSE

It is well established that in unconfining theory a bound states spectra obtained through the BSE and through the corresponding Schrödinger equation mutually agree up to the small relativistic correction. In opposite, the solution of BSE for excited states, which lie above constituents particle threshold represents a rather difficult numerical problem and no comparison is known in the literature, at least to the author.

Because of the presence of the kernel singularity, more or less standard matrix methods [25] fail since the inversion of numerical matrices is not possible. Also we do not explore more or less conventional expansion into the orthogonal polynomials which loses its efficiency when, as one expects, a relatively large number of polynoms is necessary. Instead, we solve the full two-dimensional integral equation by the method of simple iterations. For this purpose we discretize P^2 and step by step we are looking for the solution of the BSE with given P_i^2 .

The BSE for bound states is a homogeneous integral equation and it satisfies usual normalization condition. Instead of using this, to achieve a good numerical stability of the iteration process we implement normalization condition through an auxiliary function $\lambda(P)$ and solve the following equation:

$$A(p, P) = \lambda(P) \int dk_4 \int d\mathbf{k} A(k, P) G_A(k, P) K_E. \quad (14)$$

The following has been found as a particular useful choice for the function $\lambda(P)$

$$\lambda^{-1}(P) = \int dk_4 \int d\mathbf{k} A(k, P)^2 f(k, P), \quad (15)$$

where arbitrary positive weight function f was chosen to be Gaussian in \mathbf{k} and k_4 . Implementation of such $\lambda(P)$ makes BSE nonlinear but mainly numerically stable. Clearly the BSE solution has been identified when $\lambda(P) = 1$ and when the difference between consecutive iterations vanishes at the same time. We found that these two conditions happen simultaneously, while for other values of parameters P , $\lambda(P) \neq 1$ the numerics do not provide vanishing difference between iterations.

Numerical convergence of $\lambda \rightarrow 1$ depends on the density of the integration points in the important domain of momenta. Recall here that even for 1-dim reduced BSE, see Ref. [26], a relatively large number of integration points was required in order to get a precise solution. In the presented study we are dealing with 2-dim integral equation with principal value integration, thus to achieve the same accuracy it necessarily enlarge number of integration points. Compromising between computational time and an estimated numerical error we are satisfied with the use of maximum $N_{k_4} * N_{\mathbf{k}} = 184 * 96$ Gaussian points. In order to ensure the numerical stability we varied integration

TABLE I. Spectrum obtained for various number of mesh points $N = 32, 58, 72, 96$ used at each single integral. The density of mesh point is regulated by $\Lambda = 1000$ GeV and infrared regulator $\epsilon = 0.03$ GeV is used, λ and the iteration error σ are displayed for completeness. There is one more state observed at 3.880 (0.998, $2.5E - 07$) for $N = 58$, which is skipped in the table for better comparison. $M_{J\Psi} = 3098$ is used as a fit.

$M(32)$	$\lambda(32)$	$\sigma(32)$	$M(58)$	$\lambda(58)$	$\sigma(58)$	$M(72)$	$\lambda(72)$	$\sigma(72)$	$M(96)$	$\lambda(96)$	$\sigma(96)$
3.717	0.995	$1.2E - 06$	3.642	1.398	0.006	3.639	1.444	0.008	3.636	1.458	0.008
3.832	1.015	$1.5E - 05$	3.746	1.174	0.001	3.745	1.200	0.002	3.733	1.223	0.002
3.914	0.994	$2.0E - 06$	3.865	0.998	$2.5E - 07$	3.867	1.000	$1.7E - 09$	3.855	1.017	$1.8E - 05$
4.040	0.993	$2.5E - 06$	3.999	1.027	$4.5E - 05$	3.996	0.979	$2.6E - 05$	3.980	0.985	$1.23E - 05$
4.151	0.983	$1.7E - 05$	4.061	1.020	$2.5E - 05$	4.049	0.983	$1.7E - 05$	4.033	1.01	$2.24E - 05$
4.289	1.012	$1.0E - 05$	4.177	1.024	$3.7E - 05$	4.168	1.002	$3.5E - 07$	4.149	1.00	$5.24E - 06$
4.458	1.024	$3.7E - 05$	4.277	1.030	$5.7E - 05$	4.262	1.002	$3.5E - 07$	4.243	1.01	$2.03E - 05$
4.604	1.025	$4.0E - 05$	4.402	1.013	$1.1E - 05$	4.340	0.977	$3.1E - 05$	4.365	1.02	$1.3E - 05$
4.840	1.017	$1.8E - 05$	4.549	0.992	$3.5E - 06$	4.530	0.980	$2.4E - 05$	4.503	1.02	$1.4E - 05$
5.008	1.021	$1.8E - 05$	4.690	0.998	$1.4E - 07$	4.671	1.007	$3.98E - 06$	4650	1.005	$5.1E - 06$
5.318	0.989	$7.00E - 06$	4.890	0.99	$1.4e - 07$	4871	1.01	$2.07E - 05$			
5.518	1.009	$5.5E - 06$	5.055	0.998	$1.4E - 07$	5.030	1.009	$5.09E - 06$			
5.934	1.018	$2.1E - 05$	5.337	1.013	$1.0E - 05$	5.308	1.01	$1.20E - 05$			
6.171	1.015	$1.5E - 05$	5.527	0.987	$9.8E - 06$	5.496	1.02	$2.60E - 05$			
6.728	0.998	$1.6E - 07$	5.909	0.97	$3.5E - 05$						
...	6.140	1.00	$2.5E - 06$						

volume (in p -space) and the number of points as well. In order to get optimal density of integration points the upper boundary Λ is introduced in momentum integrations. More precisely, for the variable \mathbf{k} we map single integration interval $(0, 1)$ into $(0, \Lambda)$ by simple rescaling [and $(-1, 1)$ into $(-\Lambda, \Lambda)$ for variable k_4]. To assure convergence $\lambda \rightarrow 1$ the density is varied such that for lower states smaller Λ is used, while highly excited states are better obtained within higher Λ , with some cost of numerical precision in the latter case. The numerical dependence on N is shown in Table I. We also compare with the experimental data in Table II and Fig. 1. For the purpose of brevity we do not discuss all numerics here leaving more detailed discussion elsewhere. However, we can mention that as a numerical test we have checked the numerical method against the scalar

TABLE II. Comparison with PDG data (second column) and calculated spectrum. Quantum numbers correspond with assumed quantum mechanical assignment [12].

M_{96}	PDG	n, l
3097	3097	1s
3640	3686	2s
3730	3772	1d
3850	...	
3980	...	
4030	4039	3s
4150	4153	2d
4240	4263	4s
4360	4361	3d
4450	4421	5s

models [27], where the resulting BSE spectra have been already obtained by different (and in fact more accurate) method. Thus we solve 2-dim BSE on a grid given by the component of relative momentum k_4 and \mathbf{k} within the procedure described above, which provides the spectra within $\approx 1/N\%$ accuracy (N is number of points in the single, say \mathbf{k} -integration). As the regulator ϵ is implemented here, we expect the accuracy of excited vectors spectrum studied here could be comparable with the one of scalar models solutions. In our case we estimate the 1% numerical error in determination of bound state masses. Such numerical error is considerably smaller than the expected amount of energy shift due to the open threshold effects (effect associated with D meson production, not be confused with unphysical quark-antiquark threshold. An open charm is impossible to incorporate in the formalism of homogeneous BSE and it is completely ignored here).

For clarity we restrict ourself to the dynamics of charmonia in this paper. The numerical values of the models are the following

$$\begin{aligned}
 C &= 5.418 \text{ GeV}^2; & \alpha_s &= g^2/(4\pi) = 0.2 \\
 m_c &= 1.5615 \text{ GeV}; & \mu &= \mu_g = 364.35 \text{ MeV}
 \end{aligned}
 \tag{16}$$

and we use the experimental J/Ψ mass to fine-tune the correct scale at the end (in units where $m_c = 1.5$; $C = 5$ we have $M(J/\Psi) = 2975$). In order to improve the numerical stability the infrared regulator in (10) was adjusted as $\epsilon = 0.03$ GeV (for $\Lambda = 1000$ GeV, ϵ value is taken slightly larger than the smallest interval between integration points of the variable k_4).

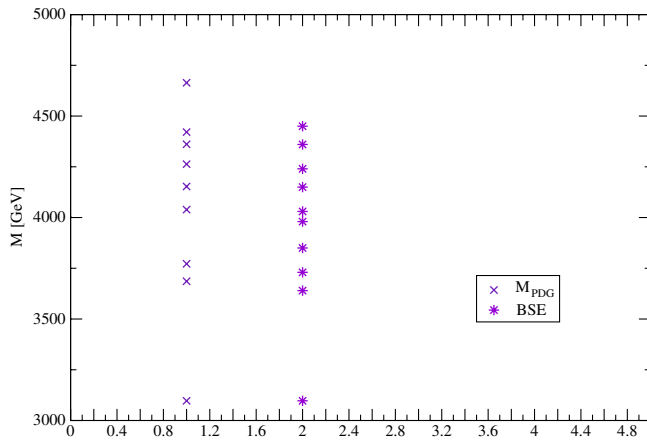


FIG. 1 (color online). Comparison of BSE solution with PDG data for vector charmonium.

As one sees from the Table I, numerically $\lambda \neq 1$ for the first two states. In fact λ do not cross unit value, instead it possesses local minima, which are stated in the Table. Further, when comparing with the experimental data, there are two more BSE solutions with masses in between ψ'' and ψ''' , while the rest of calculated excited states quite nicely agree with the data. We have not found a simple way (by varying parameters C , α , μ , m_c) to exclude these two additional states from the solutions and we suggest the reason why they are here in the section below.

IV. CONCLUSION AND DISCUSSION OF THE RESULTS

We have formulated Lorentz covariant model for vector quarkonia, which is based on the BSE with phenomenological kernel. With aforementioned exception of two additional states, the resulting spectrum is comparable with the experiments whenever the experimental data are available. The agreement between our results for higher states and the one measured in the experiments is impressive, the remaining difference between theory and experiments is due to the approximations, e.g., due to the interplay of quark and D , D^* esonic degrees of freedom, such couple channel effects are difficult to incorporate into the Bethe-Salpeter analysis presented here.

The ground state is situated near below the naive quark-antiquark threshold, while the all excited states lie above this threshold. We argue two more states which appear are the artefact of inappropriate usage of free quark propagators. The question of confinement is beyond the scope of the presented work, however we expect some changes when confinement is correctly incorporated. First of all, we expect the quark propagators should not have a free particle pole and therefore the BSE could not possess ordinary threshold singularity in this case. In the paper we are dealing with BSE where the propagators describe free—instead of confined—quarks. Therefore the threshold singularity unavoidably

appears as an artefact here. The lowest lying excited charmonia are the one closest to the naive quark-antiquark threshold and we naturally must expect some defect in the calculated spectrum. Here, very likely it leads to the mentioned appearance of two more excited states that we cannot find in the PDG, (for a recent attempt to find more definite answer see Ref. [22]).

The model presented is very simple: The BSE kernel consists from vectorial effective one gluon exchange and from the scalar infrared enhanced—double pole—interaction. A possible vector-scalar admixture of “confining” interaction has not been considered and we expect it must be small in order to suppress large hyperfine splitting. The string breaking mechanism is incorporated through the screening mass μ which is found to be comparable to Λ_{QCD} in our BSE study. The presence of Lorentz scalar interaction complemented by vector-vector interaction kernel appears to be a very important part of the model. No individual—scalar nor vector—interactions provide quarkonium spectrum [28].

Nonrelativistic quantum mechanical limit of the scalar interaction is given by the exponential potential. Consequently the spectrum of radially excited states do not correspond with linear Regge trajectory but the gap between the states increase with the mass of the bound states. This is in very good agreement with recent experiments. The intercept—the gap between J/Ψ and the first excited state $\Psi(2S)$ is driven by the interplay of the strength of vectorial and scalar interaction. As we have checked numerically, the coulombic term can be regarded as a perturbation only for existing energy levels for which it slightly shifts existing energy levels. On the other side, its omission would lead to the appearance of new states below existing $2S$ mass. We found that the correct adjustment of the energy intercept is a major effect of the effective one gluon exchange interaction. The running coupling is fixed here and its numerical value differs significantly from the one known from quantum mechanical phenomenology (it is more than two times smaller). At present stage we have no simple explanation of this fact. If our results are considered seriously then it can suggest that the average of typical square of gluon four-momenta inside quarkonium can be considerably larger than naively expected from the Schrödinger equation. A possible explanation is that the soft gluon mass is larger than the value we consider here, $\mu_g = 700\text{--}800$ MeV, however quantum mechanical limit has not yet been studied in such case. Further, comparing with the expected quantum mechanical limit then Bethe-Salpeter string breaking scale $\mu \approx 350$ MeV appears to be relatively larger than the one used in potential model $\mu \approx 150$ MeV [10,11].

There is another challenging aspect of this problem, as most of the Schwinger-Dyson equations—BSE studies rely on the ladder truncation of the equations system. After the inclusion of running quark masses, renormalization wave

functions, the techniques can be very useful in calculation of heavy-light and light flavored mesons as well. We also expect that the knowledge of off-shell behavior (e.g., $q.P$ dependence) of the amplitudes is important in various

hadronic processes. Because of this it is worthwhile to extend our study to the more complete calculations, which open possible first principle calculation of production and decay mechanisms of heavy flavor hadrons.

-
- [1] D. V. Bugg, *Phys. Rep.* **397**, 257 (2004).
 - [2] S. S. Afonin, *Phys. Lett. B* **639**, 258 (2006).
 - [3] L. Y. Glozman, *Phys. Rep.* **444**, 1 (2007).
 - [4] The large degeneracy is clear in Fig. 1 of Ref. [2] b and in Fig. 2 of Ref. [3].
 - [5] E. Aker *et al.* (Crystal Barrel Collaboration), *Nucl. Instrum. Methods Phys. Res., Sect. A* **321**, 69 (1992).
 - [6] K. G. Wilson, *Phys. Rev. D* **10**, 2445 (1974).
 - [7] E. Eichten, K. Gottfried, T. Kinoshite, K. D. Lane, and T. M. Yan, *Phys. Rev. D* **17**, 3090 (1978); **21**, 313(E) (1980).
 - [8] G. S. Bali, *Phys. Rep.* **343**, 1 (2001).
 - [9] J. Greensite and S. Olejnik, *Phys. Rev. D* **67**, 094503 (2003).
 - [10] B.-Q. Li and K.-T. Chao, *Phys. Rev. D* **79**, 094004 (2009).
 - [11] K. T. Chao and J. H. Liu, in *Proceedings of the Workshop on Weak Interactions and CP Violations, Beijing, 1989* (World Scientific, Singapore, 1990)
 - [12] P. Gonzales, V. Mathieu, and V. Vento, *Phys. Rev. D* **84**, 114008 (2011).
 - [13] E. van Beveren and G. Rupp, [arXiv:1005.3490](https://arxiv.org/abs/1005.3490).
 - [14] P. Bydzovsky and Yu. S. Surovtsev, [arXiv:0711.4748](https://arxiv.org/abs/0711.4748).
 - [15] T. Goldman and R. Silbar, *Phys. Rev. C* **85**, 015203 (2012).
 - [16] A. C. Aguilar, D. Binosi, and J. Papavassiliou, *Phys. Rev. D* **84**, 085026 (2011).
 - [17] D. Binosi and J. Papavassiliou, *Phys. Rep.* **479**, 1 (2009).
 - [18] A. Cucchieri and T. Mendes, *Phys. Rev. D* **81**, 016005 (2010).
 - [19] A. Yu. Dubin, A. B. Kaidalov, and Yu. A. Simonov, *Phys. At. Nucl.* **56**, 1745 (1993); *Yad. Fiz.* **56**, 213 (1993); A. Yu. Dubin, *Phys. Lett. B* **323**, 41 (1994); Yu. S. Kalashnikova, A. V. Nefediev, and Yu. A. Simonov, *Phys. Rev. D* **64**, 014037 (2001).
 - [20] P. C. Tiemeijer and J. A. Tjon, *Phys. Rev. C* **48**, 896 (1993).
 - [21] W. Lucha, *AIP Conf. Proc.* **1317**, 122 (2011); for further 3d reduction of BSE see: Kadyshevsky, *Nucl. Phys.* **B6**, 125 (1968); Gross, *Phys. Rev.* **186**, 1448 (1969); *Phys. Rev. C* **26**, 2203 (1982).
 - [22] V. Sauli, [arXiv:1207.2621](https://arxiv.org/abs/1207.2621).
 - [23] H. Bethe and E. Salpeter, *Phys. Rev.* **84**, 1232 (1951); Y. Nambu, *Prog. Theor. Phys.* **5**, 614 (1951).
 - [24] H. J. Munczek and P. Jain, *Phys. Rev. D* **46**, 438 (1992); P. Jain and H. J. Munczek, *Phys. Rev. D* **48**, 5403 (1993).
 - [25] M. Blank and A. Krassnigg, *Comput. Phys. Commun.* **182**, 1391 (2011).
 - [26] R. Alkofer and S. Ahlig, *Ann. Phys. (N.Y.)* **275**, 113 (1999).
 - [27] V. Sauli and J. Adam, *Phys. Rev. D* **67**, 085007 (2003).
 - [28] V. Sauli and P. Bicudo (unpublished).